Waveform Diversity and Design (WDD)

Cover Story Preface

Andy Drozd, President EMC Society

This section of the newsletter provides an article on the background of Waveform Diversity and Design (WDD) by Dr. Eric Mokole of the Naval Research Laboratory. Also included is a mission statement. These are followed by two technical articles that present some of the key technical issues and concerns confronted by this community and how EMC fits in.

The first article is titled, "Space-Time Adaptive Processing and Electromagnetic Compatibility for Waveform Diverse Distributed Aperture Radars" by Raviraj S. Adve of the Department of Electrical and Computer Engineering at the University of Toronto, Russell Brown and Richard A. Schneible of Stiefvater Consultants in Marcy, NY, Michael C. Wicks of the US Air Force Research Laboratory, Sensors Directorate in Rome, NY, and Robert McMillan of the US Army SMDC in Huntsville, AL. Their article discusses the fundamental WDD problem and the importance of having viable interference models to address relevant electromagnetic environment effects and EMI for a system of systems. Their paper furthers the development of EMC and signal processing for distributed, waveform diverse antenna arrays. The long-term goal is to develop practical waveform-time-space adaptive processing algorithms for distributed apertures. A crucial issue identified in previous works is that, in practice, the target and interfering sources are within the near-field of the antenna array. As a first step toward the long-term goal, their paper develops the model required to generate simulated data. Such a model would be particularly useful to develop and test new adaptive signal processing algorithms. Specifically, this paper develops a model for range dependent target and interference for distributed, frequency diverse apertures.

The second article is titled "Capacity Analysis of Spectrally Overlapping Direct-Sequence Spread Spectrum (DSSS) Channels" by Ilteris Demirkiran of Embry-Riddle Aeronautical University in Daytona Beach, FL, Donald Weiner and Pramod Varshney of Syracuse University in Syracuse, NY and, yours truly. In this article, concerns the exponentially burgeoning cellular business over the last decade are addressed. With the huge increase in the number of cellular users, capacity of the existing cellular system has become an issue. This is a related concern within the WDD community, i.e. there is a need to ensure that multiple cooperative radar and communications systems are operational and available across the entire electromagnetic spectrum within the application environment. In this paper, a novel approach is presented that provides for a significant increase in the number of users based on applying direct sequence spread spectrum (DSSS) waveforms, which can assist in facilitating interference-free operation. If you have questions or comments, please contact yours truly, Andy Drozd, at a.l.drozd@ieee.org.

Mission Statement Waveform Diversity and Design

The mission of the Waveform Diversity and Design community is to form a validated technology base that will take advantage of the new flexibility in waveform design and application afforded by recent and emerging advances in electromagnetics, processing, and radio frequency analog devices. This technology would then be used to pursue research, development, and production of sensors, communication, and countermeasure sensors that dynamically and harmoniously utilize multiple transmit and receive signal sets from one or more platforms to exchange and/or extract information. Workshops and conferences are vehicles for fostering the continued growth of waveform-diversity concepts and encourage the participation and contributions of outside organizations to address problems of common interest.

[Note from the EMC Newsletter Editorial staff: The Charter of the EMC Society historically has advanced technologies that "dynamically and harmoniously" permit multiple users to simultaneously operate radio frequency transmitters without detrimental effects.]

Background on Waveform Diversity and Design and Relevant Electromagnetic Interference and Spectrum Utilization Issues

by Dr. Eric L. Mokole, Naval Research Laboratory, Washington, DC

The genesis of the Tri-Service Waveform Diversity Working Group and the subsequent two IEEE conferences on Waveform Diversity and Design sprung from the fertile mind of Michael C. Wicks of the Air Force Research Laboratory (AFRL) in Rome NY. In early spring of 2002 at a meeting of the joint university-industry-government CHSSI1 team for the parallelization of WIPL-D2 in Utica, NY, he requested a side meeting with the other two service representatives, Robert W. McMillan of the US Army Space and Missile Defense Command (SMDC) and Eric L. Mokole of the Radar Division of the Naval Research Laboratory (NRL), to discuss the notion of jointly pursuing a long-term roadmap for research and development in the broad area of Waveform Diversity (WD), roughly defined as:

The dynamic and coordinated use of multiple transmit and receive signal sets from one or more platforms to exchange and/or extract information.

Over the next several months, the three principals formed a Core Team for what would become the Working Group and conducted several meetings, culminating in the 1st Tri-Service Waveform Diversity Workshop at NRL in Washington DC from February 4-7, 2003. The original Core Team had six members (Peter Kirkland of SMDC, Paul Antonik of AFRL, Karl Gerlach of NRL, and the three founding members), and the Working Group consisted of Shannon Blunt of NRL, Michael Dorsett and John Hennings of SMDC, Todd Hale of the Air Force Institute of Technology, and Patricia Woodard, Robert Bonneau, and Richard Schneible of AFRL.

In light of existing and expected RF technologies in the 2005-2009 time frame, the goals of the Working Group were to develop analytical methodologies and new hardware technologies for system applications in sensors, communications, and countermeasures. Hardware advances in electromagnetics, waveform generation, timing and control, and signal/data processing have greatly increased the performance of RF devices, which allow significantly more flexibility in modulating radar and communications signals. This improved flexibility, coupled with dynamic reprogrammability, results in the capability of generating adaptive waveforms that optimize a user's specific application. Moreover, improved analog-to-digital converters and integrated analog circuitry allow direct digital synthesis of signals without the need for complex mixing stages and baseband processing. Finally, the phase accuracies in these transceivers improve system performance in the temporal and spatial domains. These technological advances in processing and device design are what make waveform diversity possible, but at the same time, create the possibility of electromagnetically-rich environments and the potential for adverse electromagnetic environmental effects to occur. As a consequence, a validated technology base is required that takes advantage of the new flexibility afforded by recent advances in processing and RF analog design and which looks at the potential electromagnetic environment impacts.

Table 1.

EVENT	DATES	LOCATION
Working Group Created	March 28, 2002	Utica, NY USA
1st Workshop	February 4-7, 2003	Washington, DC USA
2nd Workshop	February 2-4, 2004	Verona, NY USA
1st Conference	November 8-10, 2004	Edinburgh, Scotland UK
3rd Workshop	March 15-16, 2005	Huntsville, AL USA
2nd Conference	January 22-27 2006	Lihue, HI USA
4th Workshop	November 14-15, 2006	Washington, DC USA
3rd Conference	June 11-15, 2007	Pisa, Italy

The two basic ideas behind the first workshop were:

(1) to gather a selected group of experts from academia, government, and industry to provide a knowledge base on Waveform Diversity for the Core Team; and

(2) to use this knowledge base to draft a comprehensive roadmap for developing an integrated, multi-organizational, experiment/demonstration plan to validate the predicted improvements in performance that would support a variety of new system constructs related to adaptive waveform technology.

Approximately 120 persons attended the first workshop, with participation from Australia and the United Kingdom. The significant interest generated by the workshop lead to support by Joseph Guerci of DARPA and to discussions about expanding the Working Group and conducting an international conference. Chris J. Baker of University College London and Vincent J. Amuso of Rochester Institute of Technology were selected as co-chairs for the conference that would take place in Edinburgh, Scotland from November 8-10, 2004. A member of the newly expanded Working Group, Murali Rangaswamy of AFRL, spearheaded an effort that resulted in the award of a Multi-University Research Initiative from the Air Force Office of Scientific Research on Waveform Diversity in 2005.

The primary objective of subsequent workshops was to foster the continued growth of waveform-diversity concepts. Although the initial meetings of the Working Group were predominantly radar centric, the scopes of subsequent gatherings expanded to include the broad array of disciplines encompassed by the working definition of Waveform Diversity (WD). For example, at the most recent WD gathering (2nd International Waveform Diversity and Design Conference, Lihue, HI USA) in January of 2006, special sessions were devoted to the IEEE Societies on Antennas and Propagation, Electromagnetic Compatibility, Geoscience and Remote Sensing, and Signal Processing. Thus far, three workshops and two conferences have been conducted, with a workshop and a conference scheduled within the next year (Table 1).

From the EMC/EMI perspective, the electromagnetic spectrum has become increasingly crowded in recent years. Efficient use of bandwidth is essential to meet the needs of a wide variety of technological disciplines that utilize waveform design. The importance of waveform design and specification for communication and sensor systems has long been recognized. However, it is only relatively recent advances in hardware technology that are enabling a much wider set of design freedoms to be explored. The need for this exploration is increased by emerging and compelling changes in system requirements, such as more efficient use of the electromagnetic spectrum, higher sensitivities, greater information content, and improved tolerances to errors. The combination of hardware advances and more stringent requirements is fuelling worldwide interest in the subject of waveform design and the use of waveform-diversity techniques.

References:

[1] The Common HPC Software Support Initiative (CHSSI), entitled Parallel Scene Generation/Electromagnetic Modeling of Complex Targets in Complex Clutter and Propagation Environments, of the High Performance Computer Modernization Office (HPCMO).

[2] B. Kolundzija, J. S. Ognjanovic, and T. K. Sarkar, WIPL-D: Electromagnetic Modeling of Composite Metallic and Dielectric Structures — Software and User's Manual (Artech House, Norwood, 2000).

Space-Time Adaptive Processing and Electromagnetic Compatibility for Waveform Diverse Distributed Aperture Radars

Raviraj S. Adve[*] *Russell Brown* *Richard A. Schneible*[†] *Michael C. Wicks*[‡] *Robert McMillan*[§]

**Dept. of Elec. and Comp. Eng., University of Toronto, 10 King's College Rd, Toronto, ON M5S 3G4, Canada, rsadve@comm.utoronto.ca*

†Stiefvater Consultants, 10002 Hillside Terrace, Marcy, NY 13403, USA.

‡ US Air Force Research Lab., Sensors Dir., 26 Electronics Pkwy., Rome, NY 13441, USA.

§US Army SMDC, 106 Wynn Drive, Huntsville, AL 35805, USA.

Keywords: Distributed apertures, frequency diversity, range-dependent clutter, electromagnetic environments

Abstract

This paper furthers the development of electromagnetic compatibility and signal processing for distributed, waveform diverse, antenna arrays. The long-term goal is to develop practical waveform-time-space adaptive processing algorithms for distributed apertures. A crucial issue identified in previous works is that, in practice, the target and interfering sources are within the near-field of the antenna array. As a first step toward the long-term goal, this paper develops the model required to generate simulated data. Such a model would be particularly useful to develop and test new adaptive signal processing algorithms. Specifically, this paper develops a model for range dependent target and interference for distributed, frequency diverse, apertures.

Compared to conventional radars, distributed aperture radars have the potential to provide significantly improved detection, tracking and discrimination performance in severe EMI and clutter environments. Realizing this greater capability will require unique waveform selection and signal processing approaches, this paper presents the development and validation of a computer simulation capability that will permit the analysis of these waveforms and interference rejection algorithms for DAR systems. For example, distributed aperture radars can potentially provide significantly improved target tracking accuracy because of the large baseline between the various apertures. The resulting angular resolution can be orders of magnitude better than the resolution of a monolithic system (single large radar). The same angular resolution can provide improved interference rejection. A high-fidelity sensor simulation was developed and was employed to investigate EMI rejection for various distributed aperture radar concepts. A waveform/processing approach using simultaneous orthogonal waveforms was shown to effectively reject EMI from all angles. An experimental program has been accomplished to validate the simulation.

1. Introduction

In the field of radar signal processing, a recent exciting approach has been to combine the benefits of extremely sparse arrays with the benefits of waveform diversity. Such a system is based on an array of sub-apertures placed several thousands of wavelengths apart. Waveform diversity has been proposed to deal with the resulting problems of grating lobes. Each sub-aperture of the array transmits a unique waveform, orthogonal to waveforms transmitted by the other apertures, preventing fratricide and maintaining electromagnetic compatibility across the distributed aperture. Initial studies have shown that while providing a remarkably narrow mainbeam, such a system can also eliminate grating lobes [1, 2].

So far, research into waveform diverse distributed apertures has mainly been for proof-of-concept. In the area of adaptive signal processing for such systems, in particular, the studies have been limited and very preliminary [1, 3]. The approach in these studies was to apply the existing space-time-adaptive processing (STAP) algorithms to the waveform-time-space adaptive processing (WTSAP) case. Waveform diversity is achieved using multiple narrow band transmissions. While the results were promising, in general, the studies serve more to highlight the work remaining in developing practical adaptive processing for waveform diverse distributed apertures.

A very important result that came out of the recent work [1, 2], is that given the extremely long baselines (thousands of wavelengths), the ranges of interest are not in the far field of the antenna array, indeed the entire notion of steering vector has to be revisited. The range dependence of target and interference has a significant impact on the performance of adaptive algorithms and requires the formulation of algorithms specifically to address this issue.

In developing adaptive signal processing for airborne radar arrays, a crucial development was the availability of data models for the target and interference [4]. This paper attempts to make a similar contribution for frequency diverse, distributed apertures, developing a model for range dependent target and interference, including frequency diversity. To account for the frequency diversity, the processing scheme uses a true time delay between the widely distributed apertures. The interference is modeled as a sum of several low power interference sources, each with range dependent contribution to the overall interference. This paper also presents numerical simulations using this model to generate data. The examples demonstrate the importance of frequency diversity in eliminating grating lobes. It is anticipated that the model will help jump-start the development of WTSAP algorithms specifically for waveform diverse distributed apertures.

This paper is organized as follows: Section 2 presents the model for range dependent target and clutter data, including

true time delay. Section 3 presents some numerical examples illustrating range dependence and the importance of frequency diversity in eliminating grating lobes. Finally, Section 4 draws some conclusions and points to future work

2. Data Model

In the case of airborne radar, the development of the data model depends heavily on the notion of a steering vector, the vector of signals at the ports of receiving antenna array due to a single source [4]. Because the sources are in the far-field, the steering vector, usually an array of phase shifts, depends only on the angle between the source direction and the array baseline. Adaptive processing techniques depend heavily on the availability of the target steering vector.

The situation is not as simple for distributed arrays. Given an antenna array with largest dimension D, operating at wavelength λ, the distance to the far field must satisfy three criteria [5]:

$$r \gg D, \quad (1)$$

$$r \gg \lambda, \quad (2)$$

$$r \gg 2D^2/\lambda. \quad (3)$$

Using typical values for distributed apertures, D=200m, λ= 0.03m, implies that the far field begins at a distance of approximately 2700km. Clearly both targets and interfering sources are not in the far field. This fact requires that any analysis of waveform diverse apertures start "from scratch". The notion of steering vector still exists, but now depends on both angle and range, i.e., each point in space corresponds to in its own steering vector. Furthermore, coherent processing of the signals over the distributed array with frequency diversity requires true time delays, as opposed to the phase shifts used in narrowband processing. Formulating the steering vector requires accounting for all these issues.

2.1 System Model and Steering Vector

The abstract model of the distributed aperture using frequency diversity is as follows: The array is assumed to comprise N elements distributed over the x - y plane, at points (x_n, y_n), n =1,...,N. Each element in the array transmits a coherent stream of M linear-FM pulses, with common bandwidth B with pulse repetition interval (PRI) Tr. However, each element transmits at a different central frequency f_n, n = 1,...N. The transmission scheme uses true time delay to focus on a look-point (X_t, Y_t, Z_t). This is in contrast to airborne radar wherein a transmitting array uses phase shifts to transmit in a look direction. The return signal at all N frequencies is received and processed at all N elements, i.e., the return signal over space, time and frequency can be written as length N^2M vector.

The receiver uses true time delay to coherently process all N frequencies. Denote as

$$D_n = \sqrt{(X - x_n) + (Y - y_n) + (Z - z_n)^2},$$

the distance of the look point to the n^{th} element. The time delay used the nth element on receive is

$$\Delta T_n = \frac{\max\{D_n\} - D_n}{c}, \quad (4)$$

GET READY FOR THE NEXT WAVE IN EMI RECEIVERS

The CER2018 Compliant Emissions Receiver is here. And in many ways it's unlike any receiver that came before it.

This complete EMI test solution offers continuous coverage from 20 Hz to 18 GHz with expandability to 110 GHz. And to ensure the highest accuracy, it self-calibrates on-demand at every frequency scan.

It includes a built-in computer that operates under Windows XP. Software is also included free along with a 19" flat screen monitor, keyboard and mouse. Programmed-in test formats include CISPR 16-1-1, MIL-STD 461/462, ANSI C63 and FCC. All functions are menu-driven. There is no need to fiddle with switches, buttons or sliders.

Like all AR Worldwide products, the CER2018 is backed by the best and most comprehensive warranty in the business. AR Worldwide is here to help you – today, tomorrow and always.

To learn more, visit us at www.ar-worldwide.com or call an applications engineer at 800-933-8181.

ar worldwide
receiver systems
rf/microwave instrumentation • modular rf • receiver systems • ar europe
Copyright© 2006 AR Worldwide. The orange stripe on AR Worldwide products is Reg. U.S. Pat. & Tm. Off.

where c is the speed of light. This is the time delay introduced to the signal at the n^{th} receive element. By using true time delay, the normalized response at the N elements due to all N frequencies for a target at the look point is just a vector of ones, i.e., the space-time-frequency steering vector, s, is given by

$$\begin{aligned} \mathbf{s} &= \mathbf{s}_t \otimes \mathbf{s}_{sf}, && (5)\\ \mathbf{s}_t &= \left[1, e^{j2\pi f_d T_r}, \ldots, e^{j(M-1)\times 2\pi f_d T_r}\right]^T, && (6)\\ \mathbf{s}_{sf} &= [1, 1, 1, \ldots, 1]^T, && (7) \end{aligned}$$

where $\otimes$ denotes the Kronecker product, f_d the target Doppler frequency, st the length-M temporal steering vector as in [4] and s_{sf} the length-N^2 space-frequency steering vector of ones.

2.2 Interference Model

As in the case of airborne radar [4], interference here is modeled as the sum of many low power sources. However, due to frequency diversity and true time delay, interference model is far more complex than in the airborne radar case. We begin by deriving the contribution for an individual interference source for one frequency f_n. The transmitted signal over M coherent pulses with pulse shape $u_p(t)$ is given as

$$s(t) = u(t)e^{j2\pi f_n t+\psi}; u(t) = \sum_{m=0}^{M-1} u_p(t - mT_r), \quad (8)$$

where ψ is a random phase shift. The received signal at element i due to this transmitted signal at frequency f_n is

$$\tilde{r}_i^n(t) = A_c u(t - \tau_i)e^{j2\pi(f_n+f_{dc})(t-\tau_i)}, \quad (9)$$

where A_c is the complex amplitude, with random phase (also incorporating ψ) f_{dc} the Doppler frequency of the interference source and

$$\tau_i = \left(\sqrt{\left(x_i - x^l\right)^2 + \left(y_i - y^l\right)^2} + \left(z_i - z^l\right)^2\right)/c$$

is the delay from the l_{th} interference source to the i_{th} element. After down-conversion and delaying the signal by ΔT_i, the baseband signal at element i is

$$\begin{aligned} r_i^n(t) &= A_c u(t - \tau_i - \Delta T_i)e^{-2\pi f_n(\tau_i+\Delta T_i)} \\ &\times \quad e^{j2\pi f_{dc}t}e^{-j2\pi f_{dc}(\tau_i+\Delta T_i)}. \quad (10) \end{aligned}$$

After matched filtering with the time reversed pulse shape, the signal becomes

$$\begin{aligned} x_i^n(t) &= \int_{-\infty}^{\infty} r_i(\tau)u_p^*(\tau - t)d\tau, && (11)\\ &= \sum_{m=0}^{M-1} A_c e^{-j2\pi f_n(\tau_i+\Delta T_i)}e^{jm2\pi f_{dc}mT_r} \times \\ &\int_{-\infty}^{\infty} u_p(\tau - \tau_i - \Delta T_i - mT_r)u_p^*(\tau - t) \\ &e^{j2\pi f_{dc}(\tau-\tau_i-\Delta T_i-mT_r)}d\tau. && (12) \end{aligned}$$

The final integral is recognized as the ambiguity function of the pulse shape evaluated at the interference source Doppler f_{dc}. Therefore,

$$\begin{aligned} x_i^n(t) &= \sum_{m=0}^{M-1} A_c e^{-j2\pi f_n(\tau_i+\Delta T_i)}e^{j2\pi f_d mT_r} \\ &\chi(t - mT_r - \tau_i - \Delta T_i, f_{dc}), \quad (13) \end{aligned}$$

where $x(\tau,f)$ is the ambiguity function of the pulse shape $u_p(t)$ evaluated at delay τ Doppler f. Sampling this signal every $t = kT_s$ corresponding to each range bin and using $\chi(mT_r, f) \simeq 0, m \neq 0$,

$$\begin{aligned} x_i^n(kT_s) &= \sum_{m=0}^{M-1} A_c e^{-j2\pi f_n(\tau_i+\Delta T_i)}e^{j2\pi f_d mT_r} \\ &\chi(kT_s - mT_r - \tau_i - \Delta T_i, f_{dc}). (14) \end{aligned}$$

Finally, given N_c interfering sources at location

$$\left\{x^l, y^l, z^l\right\}_{l=1}^{N_c}$$

with corresponding Doppler frequency f_{dc}^l, , the received signal the i^{th} element on the mth pulse at frequency f_n is

$$\begin{aligned} x_i^n(kT_s, m) &= \sum_{l=1}^{N_c} A_c^l e^{-j2\pi f_n(\tau_i^l+\Delta T_i)}e^{j2\pi f_n^l mT_r} \\ &\chi(kT_s - \tau_i^l - \Delta T_i, f_{dc}^l), \quad (15) \end{aligned}$$

Note that ΔT_i, defined in Equation 4, remains the delay from the look point to the i^{th} element.

3. Numerical Simulations

This section presents the results of numerical simulations using the model developed above. In keeping with the nascent nature of this research area, the examples are preliminary in nature focusing on non-adaptive processing. They serve to illustrate the importance of frequency diversity and the need for range dependent adaptive processing. The first example illustrates the "beampattern" of the matched filter processing. Note that since the steering vector is range dependent, this is not the traditional sense of beam pattern. The second example illustrates the need for frequency diversity. The first two examples do not include any interference. The final example includes interference and illustrates the need for adaptive processing.

Table 1: Parameters common to all examples

Parameter	Value	Parameter	Value
N	16	M	8
B	10MHz	T_p	$10\mu s$
PRI	$5T_p$	Target SNR	10dB
Target Velocity	50m/s	Freq. Offset	100MHz
X_t	-86.51m	Y_t	-333.12m
Z_t	200km	INR	50dB

All examples use the same parameters, shown in Table 1. The array uses a nominal center frequency of 10 GHz. In the table, T_p refers to the duration of each linear FM up-chirp. The frequency offset is the difference between carrier frequencies of the N transmissions. The array elements are uniformly distributed in the $x - y$ plane on a square 200m x 200m grid. The interference-to-noise ratio (INR) is relevant only if interference data is included in the simulation.

3.1 Example 1: Beampatterns

The first example illustrates the transverse and "radial" beam patterns, i.e., in the x- and z- directions. Figure 1 plots the beampattern along the x-direction. The figure plots the output, using matched filtering, for various values for the transverse dimension. The figure shows that the array has an approximate

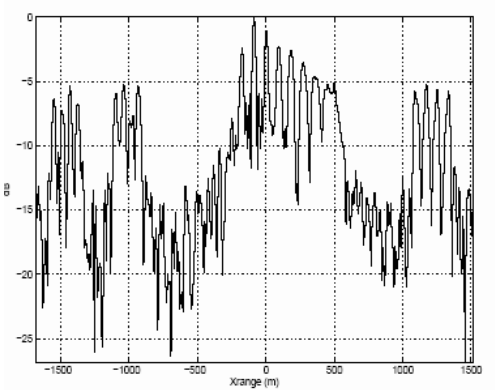

Figure 1. Matched filter processing along the transverse, x-direction.

beamwidth of 25m in the transverse direction. Note that the target is 200km distant from the array in the radial, *z*-direction.

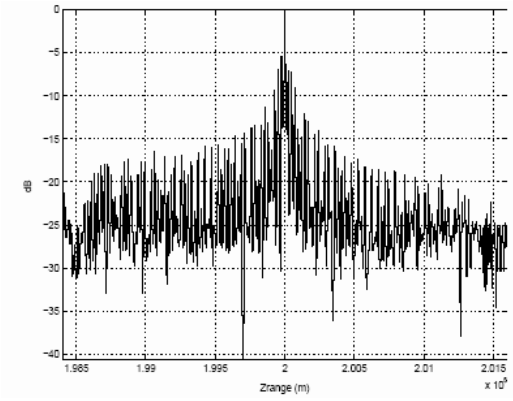

Figure 2. Matched filter processing along the radial, z-direction.

Figure 2 plots the beampattern along the radial z-direction. From the figure, the range resolution is approximately 2m. In both cases, the distributed aperture, coupled with frequency diversity, shows remarkably good resolution in both radial and transverse directions.

3.2 Example 2: Need for Diversity

This example illustrates the need for frequency diversity. Figure 3 plots the beampattern in the transverse direction. Note the closely spaced grating lobes. The range dependence of the steering vector results in a very small decay in the grating lobe level further away from the target location X^t. However, clear-

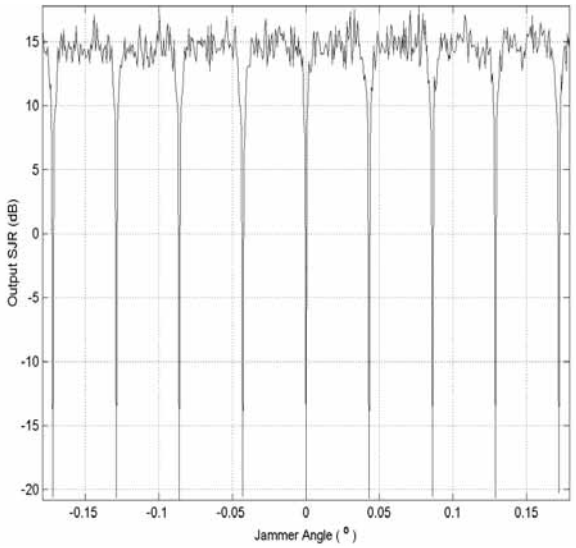

Figure 3: Matched filter processing along the transverse direction (equally spaced sub-apertures/no frequency offset).

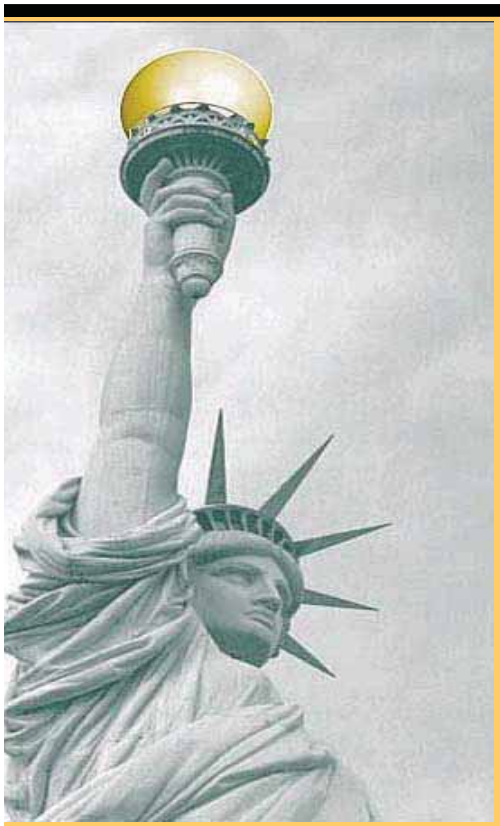

Finally...
The Freedom to have:

- ✓ *Precise antenna calibration*
- ✓ *Accurate shielding measurements*
- ✓ *Accurate test site calibration*

Precision Spherical Dipole Source

... a highly ***accurate & repeatable*** Electric field source.

Ideal for:

- ✓ commercial and government EMI/EMC test laboratory calibration measurements.
- ✓ highly **accurate and repeatable** shielding effectiveness measurements

AET
Applied Electromagnetic Technology

P.O. Box 1437, Solomons, Maryland 20688-1437
Phone: (410) 326-6278, Fax: (410) 326-6278
info@appliedemtech.com • www.appliedemtech.com

Advanced technology for accurate electromagnetic measurements

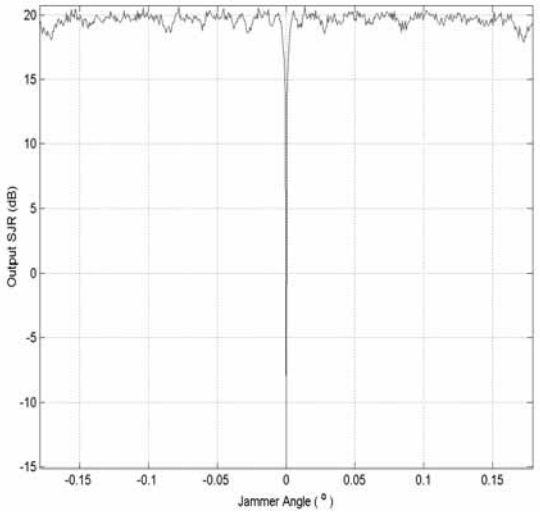

Figure 4: Matched filter processing along the transverse direction (irregularly spaced sub-apertures/frequency diversity).

ly the decay is inadequate for purposes of target detection. Figure 4 plots the beampattern in the transverse direction for an irregularly spaced sub-aperture and with frequency diversity. The combination of sub-aperture spacing and waveform diversity has eliminated the grating lobes.

Figure 5 plots the beampattern in the radial z-direction. As expected, grating lobes do not occur. However, note the significantly reduced range resolution as compared to Figure 2.

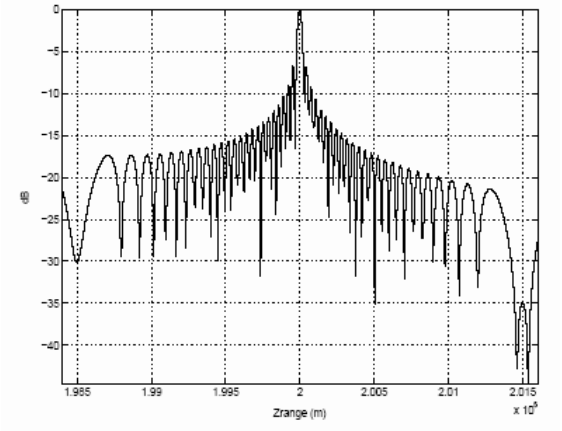

Figure 5: Matched filter processing along the radial, z-direction, no frequency offset.

3.3 Example 3: Including Interference

The final example illustrates the effect of interference. Interference is modeled as a spherical cluster of 104 low power interfering sources offset from the target location by 1.6 km. The radius of the cluster is set to 400m.

Figures 6 and 7 plot the results of non-adaptive processing. Figure 6 plots the output statistic as a function of the transverse, x-direction, while Figure 7 plots the output statistic as a function of the radial z-direction. As is clear from both figures, the strong interference completely buries the weak target.

Figure 8 plots the modified sample matrix inversion (MSMI) statistic [4] as a function of the transverse x-direction. This adaptive processing is implemented using only a single pulse, not the entire data cube. This is necessitated by the fact that the interference is spatially limited, i.e., the interference occupies only a few range cells, limiting the available secondary data for covariance matrix estimation. However, even with a single pulse, adaptive processing identifies the target within the strong interference.

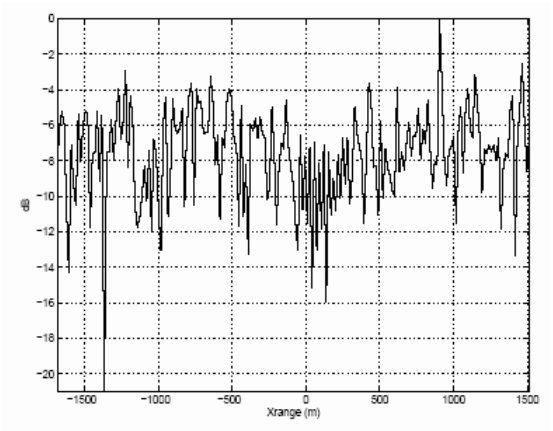

Figure 6: Matched filter processing along the transverse, x-direction, includes interference.

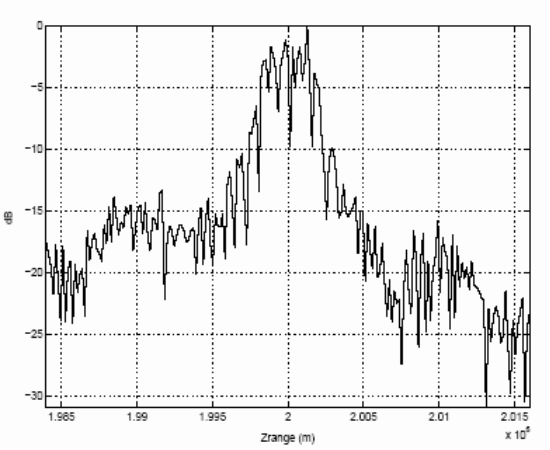

Figure 7: Matched filter processing along the radial, z-direction, includes interference.

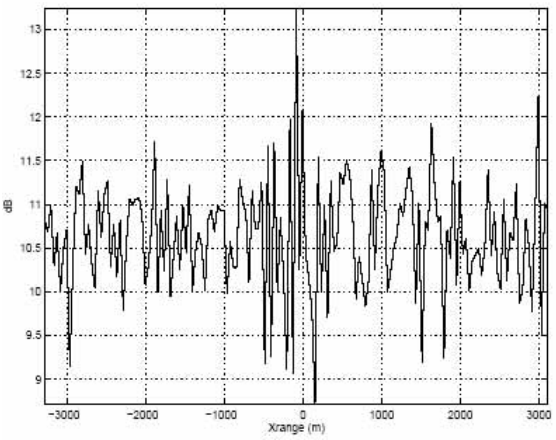

Figure 8: MSMI statistic versus transverse x-dimension, includes interference.

3.4 Experimental Verification

A distributed aperture radar system was built. Five sub-aperture systems were constructed and distributed with irregular spacing over a 250-foot aperture length. Employing a 6000-foot test range, a target was driven across the sub-aperture mainbeam and in front of an interference source. Waveform diversity was employed and the target detected close to the angle of the interference (well within the sub-aperture mainbeam). Figure 9 shows the results, which are a scaled version of those shown in Figure 4.

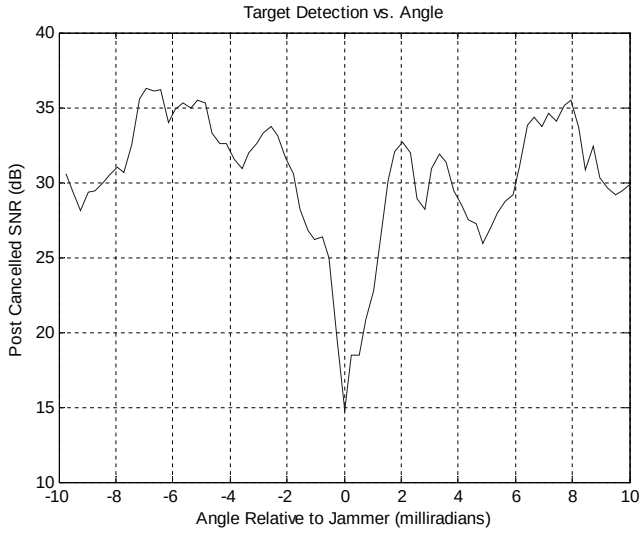

4. Conclusions and Future Work

This paper has taken the initial steps toward developing adaptive processing for distributed aperture, frequency diverse, arrays. The steps are parallel to those undertaken in the 1990s that proved successful in the development of STAP for airborne radar, starting with the development for a data model [4]. Starting from the realization that the target and interfering source are not in the far-field of the array, this paper develops a data model accounting for range dependence while accounting for true time delay for multiple frequency bands. The numerical examples illustrate the importance of having such a data model. The data model is used here to estimate the beampattern and beamwidths in both the transverse and radial directions.

The numerical results also illustrate the crucial differences from STAP for airborne radar and the work remaining to develop a good understanding of adaptive processing for distributed apertures. As the third example shows, in crucial interference scenarios of interest, the availability of secondary data is a crucial issue. It is, therefore, likely that available adaptive algorithms, developed for airborne radar, are not relevant to the application at hand. The long-term goal of this effort is the development of adaptive algorithms specifically for distributed aperture, frequency diverse, arrays. EMC

References

[1]R.S. Adve, “Adaptive processing for distributed aperture radars”, in Proc. of the 1st Waveform Diversity Workshop, Feb. 2003. NRL, Washington DC.

[2]R.S. Adve, R.A. Schneible, and R. McMillan, “Adaptive space/frequency processing for distributed apertures”, in Proc. of 2003 IEEE Radar Conference, May 2003. Huntsville, AL.

[3]R.S. Adve, “Sub-optimal adaptive processing for distributed aperture radars”, in Proc. of the 2nd Waveform Diversity Workshop, Feb. 2004. Verona, NY.

[4]J. Ward, “Space-time adaptive processing for airborne radar”, Tech. Rep. F19628-95-C-0002, MIT Lincoln Laboratory, December 1994.

[5]C. Balanis, Antenna Theory: Analysis and Design. John Wiley, 1997.

Capacity Analysis of Spectrally Overlapping Direct-Sequence Spread Spectrum (DSSS) Channels

Ilteris Demirkiran[ß], Donald Weiner[™], Pramod Varshney[™], Andrew Drozd[*]

[ß]*Electrical Engineering, Embry-Riddle Aeronautical University, Daytona Beach, FL 32114, USA.*

[™]*Electrical Engineering and Computer Science, Syracuse University, Syracuse, NY 13244, USA.*

[*]*Andro Computational Solutions, LLC, Rome, NY 13440-2067*

Abstract: It is well known that cellular business has been increasing exponentially in the last decade. With the huge increase in the number of cellular users, capacity of the existing cellular system has become an issue. In this paper, a novel approach is presented that provides for a significant increase in the number of users in multi-user DSSS Systems.

I. Introduction

Using code division multiple access (CDMA) techniques, it is possible to have multiple users which simultaneously transmit information over a single channel. This is achieved by use of a different spreading code for each user. Ideally the spreading codes in a multi-user DSSS system are orthogonal. There is then zero interference between users provided that the data streams are synchronized. However, in practice, the spreading codes are only approximately orthogonal because the number of codes that are strictly orthogonal for a given length is very limited and, in addition, the data streams of multiple users are not likely to be synchronized. As a result, the variance of the decision statistic at the output of the correlation receiver is not zero. This variance, which limits the number of users for a pre-

specified probability of error, is found to be [1]

$$\sigma^2 = \sum_{k=1}^{K_1-1} \int_{-\infty}^{\infty} [W_{s_k}(f) \otimes W_{v_o}(f)][T_{do}\mathrm{sinc}(fT_{do})]^2 df \quad (1)$$

Where $\otimes$ denotes convolution, $(K_1 - 1)$ is the number of interfering users, T_{do} is the bit duration, and $W_{sk}(f)$ and $W_{v_0}(f)$ are the power spectral densities (PSDs) of the transmitted DSSS signals and the correlating signal at the receiver, respectively, and are given by [1,2]

$$W_{s_k}(f) \approx \frac{T_{ck}P_k}{2}\{\mathrm{sinc}^2[(f-f_{ck})T_{ck}] + \mathrm{sinc}^2[(f+f_{ck})T_{ck}]\} \quad (2)$$

and

$$W_{v_o}(f) = \frac{T_{co}}{4}\{\mathrm{sinc}^2[(f-f_{co})T_{co}] + \mathrm{sinc}^2[(f+f_{co})T_{co}]\}. \quad (3)$$

T_{ck}, P_k, and f_{ck} in Eq. (2) are the chirp duration, average power, and carrier frequency of the k^{th} DSS interferer, respectively, while T_{c0} and f_{c0} in Eq. (3) are the chirp duration and carrier frequency of the desired DSSS signal, respectively. Invoking the central limit theorem, the interference statistic is modeled as a Gaussian random variable. The probability of error is then given by [1,2]

$$P_e = Q\left(\sqrt{\frac{P_o T_{do}^2}{2\sigma^2}}\right) \quad (4)$$

where, by definition,

$$Q(x) = \int_x^{\infty} \frac{1}{\sqrt{2\pi}} e^{-\frac{z^2}{2}} dz \quad (5)$$

and P_0 is the average power of the desired DSSS signal.

As seen from the interfering signal variance expression given in Eq. (1), analytical calculation of this variance is a very difficult task. The k^{th} integral involves the convolution of $W_{sk}(f)$ with $W_{v_0}(f)$, given by Eqs. (2) and (3), respectively, weighted by the square of a sinc function. Each of the power spectral densities in the convolution consists of the squares of sinc functions. Therefore, the integrand of the k^{th} integral involves products of the square of sinc functions. Closed form evaluation of such an integral is not known. However, this difficulty can be overcome by upper-bounding the squared sinc terms in the variance integral with truncated cosine squared functions. Having made this approximation, the approximated PSDs of the transmitted DSSS signals can be expressed as

$$\hat{W}_{sk}(f) = \frac{P_k T_{ck}}{2}\{cos^2[(f+f_{ck})\frac{\pi T_{ck}}{2}]\Pi(\frac{f+f_{ck}}{2/T_{ck}}) + \cos^2[(f-f_{ck})\frac{\pi T_{ck}}{2}]\Pi(\frac{f-f_{ck}}{2/T_{ck}})\}. \quad (6)$$

where the rectangular function is

$$\Pi(\frac{f}{2\omega}) = \begin{cases} 1 & -\omega \le f \le \omega \\ 0 & \text{otherwise.} \end{cases} \quad (7)$$

Using the identical reasoning that led to the approximations in Eq. (6), $W_{v_0}(f)$ and $G(f) = [T_{do}\mathrm{sinc}(fT_{do})]^2$ can be approximated in the same manner. The approximations for $W_{v_0}(f)$ and $G(f)$ are then given by

$$\hat{W}_{v_o}(f) = \frac{T_{c_o}}{4}\{\cos^2[(f+f_{co})\frac{\pi T_{c_o}}{2}]\Pi(\frac{f+f_{co}}{2/T_{co}}) + \cos^2[(f-f_{co})\frac{\pi T_{c_o}}{2}]\Pi(\frac{f-f_{co}}{2/T_{c_o}})] \quad (8)$$

and

$$\hat{G}(f) = T_{do}^2\cos^2(\frac{\pi f T_{do}}{2})\Pi(\frac{f}{2/T_{do}}). \quad (9)$$

Substitution of the approximations, defined above, into the k^{th} term in Eq.(1), the variance due to the k^{th} interferer is approximated by

$$\sigma_k^2 \approx \int_{-\infty}^{\infty} [\hat{W}_{s_k}(f) \otimes \hat{W}_{v_o}(f)]\hat{G}(f)df. \quad (10)$$

This is a general result that can be used whether or not the desired and interfering signals have the same carrier frequencies and bandwidths. Now this general result is utilized to determine the co-channel and adjacent channel interference variances, which are needed for the capacity analysis of spectrally overlapping DSSS channels.

Consider a case where a single interfering DSSS signal and the desired DSSS signal have identical carrier frequencies and bandwidths (i.e., $f_{ck} = f_{c0}$ and $T_{ck} = T_{c0}$). By using Eq.(10) the co-channel interference variance is found to be

$$\sigma_{cc,1}^2 = \frac{T_{do}^2}{16}[\frac{4L_o^6 + 4L_o^5\pi^2 - (6+\pi^2)L_o^4 - 8\pi^2L_o^3 + 2\pi^2L_o^2 + 4\pi^2L_o + 4 - \pi^2}{2\pi^2L_o^2(1-L_o^2)^2} + \frac{L_o^2(3-2L_o^2)}{\pi^2(1-L_o^2)^2}\cos(\frac{\pi}{L_o}) + \frac{L_o(1-2L_o)}{2\pi(1-L_o^2)}\sin(\frac{\pi}{L_o})]P_k \quad (11)$$

where $L_0 = T_{d0}/T_{C0}$ is the processing gain.

For adjacent channel interference variance, consider the case where a single interfering DSSS signal has the same bandwidth as the desired signal but a carrier frequency spaced half a bandwidth from the desired signal carrier frequency (i.e., $f_{ck} = f_{c0} + 1/T_{c0}$ and $T_{ck} = T_{c0}$). The adjacent channel interference variance is found to be

$$\sigma_{ac,1}^2(L_o) = \frac{T_{do}^2}{32\pi(L_o^2-1)L_o}[2\pi L_o^2 - 2\pi - L_o^3\sin(\pi/L_o)]P_k. \quad (12)$$

Having obtained the co-channel and adjacent-channel interference variances, attention is devoted to a novel technique which provides for a significant increase in the number of users in multiple-users DSSS systems. The technique is based on division of the DSSS channel into a number of sub-channels.

Consider a multiple user DSSS system assigned to a single channel of bandwidth, B_1. The maximum processing gain for each user is achieved by spreading its spectrum to fill the entire channel bandwidth. Consequently, in multiple user DSSS systems, each user has maximum bandwidth, B_1, and the same carrier frequency, f_{c0}, located at the center of the channel. For simplicity, assume each user has the same average power, P_0. Given the processing gain and the prespecified probability of error, it is possible to determine the maximum number of users. We refer to this case as having a full channel spectral allocation and denote the maximum number of users by K_1. For the same channel of bandwidth, B_1, the question arises as to whether it is possible to allocate each user's spectrum in a manner different from the full channel allocation so as to increase the number of users beyond K_1.

II. Full Channel Spectral Allocation

In order to establish the notation to be used, the full channel spectral allocation case is discussed first. This case serves as the base line. Here all users have the same bandwidth equal to the

channel bandwidth, B_1, and the same center frequency, fco. In addition, each user is assumed to have the same average power, P_0. The maximum number of users is denoted by K_1. This number is evaluated under the condition that the same pre-specified probability of error for each user is not exceeded.

Since the bandwidth of a rectangular pulse is equal to the inverse of its pulse width, the processing gain can be also expressed as

$$L_1 = \frac{B_1}{B_d} \qquad (13)$$

where B_1 and B_d are the bandwidths of the chip and data pulses, respectively. The variance due to a single interferer is given by Eq. (11). Because the interferers have the same average power and processing gain, the variance due to the $(K_1 - 1)$interferers is

$$\sigma^2_{cc,(K_1-1)}(L_1) = (K_1 - 1)\sigma^2_{cc,1}(L_1) \qquad (14)$$

where statistical independence between the users is assumed. The maximum number of users is determined by increasing K_1 to its maximum value such that the pre-specified probability of error is not exceeded.

III. Overlapping Sub-Channels

Now assume that the entire channel of bandwidth B_1 is divided into m non-overlapping sub-channels of bandwidth $Bm = B_1/m$ and $(m - 1)$ overlapping sub-channels having the same bandwidth Bm but centered at the cut-off frequencies of the non-overlapping sub-channels. Therefore, a total of $(2m - 1)$ sub-channels of bandwidth Bm subdivide the original channel of bandwidth B_1. Fig. (1) illustrates the case for which the channel of bandwidth B_1 is subdivided into four non-overlapping sub-channels (m=4) plus three (m-1=3) additional sub-channels to produce 7 overlapping sub-channels. As

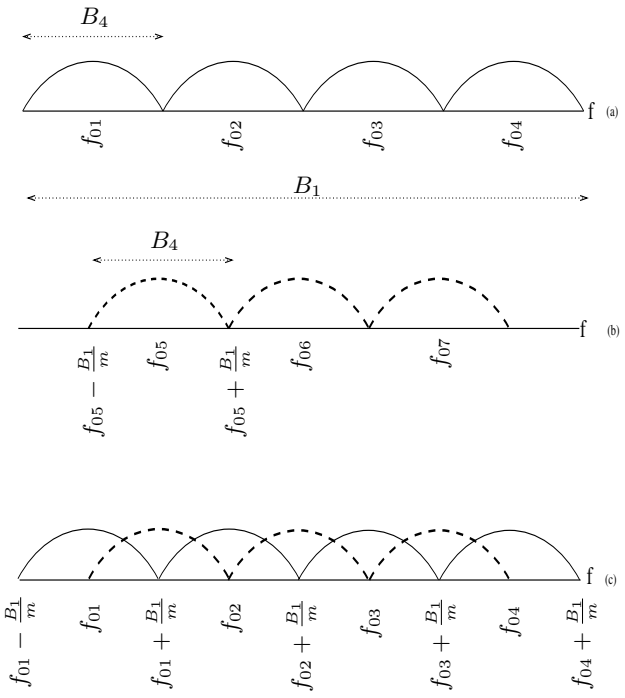

Figure 1: The case for which m=4 (a) 4 non-overlapping sub-channels (b) 3 additional sub-channels (c) 7 overlapping sub-channels can be seen from Fig. (1), a desired signal now experiences interference from both other users in the same sub-channel (i.e., co-channel interference) as well as those in the neighboring sub-channels (i.e., adjacent channel interference). For simplicity, a worst case situation is analyzed where it is assumed that all desired users suffer adjacent channel interference from the sub-channels on both sides even though the end-channels experience interference from only one side. Once again, the objective is to maximize the number of users such that the probability of error experienced by each user does not exceed the common prespecified probability of error. Using symmetry and neglecting end-channel effects, the maximum number of users allowed within each sub-channel is equal and is denoted by K_{2m-1}. Here, the subscript on K represents the presence of $(2m-1)$ sub-channels within the original channel of bandwidth B1. It follows that there are $(K_{2m-1} - 1)$ co-channel interferers and $2K_{2m-1}$ adjacent-channel interferers. Therefore, the total interference variance is

$$\sigma^2_{(tot)}(L_m) = (K_{2m-1} - 1)\sigma^2_{cc,1}(L_m) + 2K_{2m-1}\sigma^2_{ac,1}(L_m) \qquad (15)$$

where L_m is the sub-channel processing gain. Observe that each sub-channel has the same bandwidth, B_m. Consequently, the processing gain for each DSSS users is equal and is given by

$$L_m = \frac{B_m}{B_d} = \frac{B_1/m}{B_d} = \frac{L_1}{m}. \qquad (16)$$

It is of interest to plot the ratio between the variances in Eqs. (11) and (12) as a function of L_m. In particular, let

$$R_{\sigma^2} = \frac{\sigma^2_{cc,1}(L_m)}{\sigma^2_{ac,1}(L_m)}. \qquad (17)$$

This ratio is plotted in Fig. 2. From this figure, it is seen

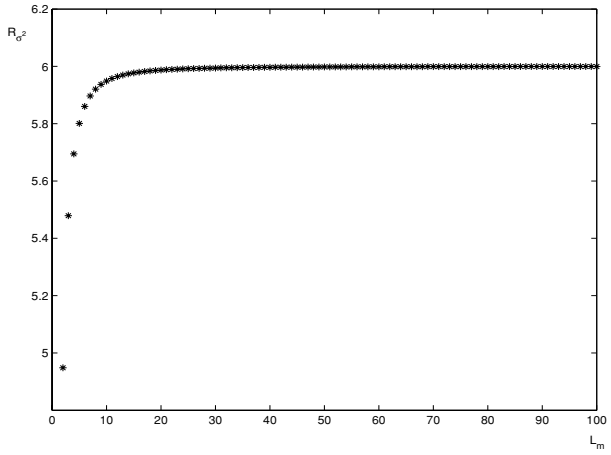

Figure 2: Plot of the ratio R_{σ^2} vs. L_m

that $R_{\sigma^2} \approx 6$ for $L_m \geq 10$.

Assuming $L_m \geq 10$

$$\sigma^2_{ac,1}(L_m) \approx \frac{1}{6}\sigma^2_{cc,1}(L_m) \qquad (18)$$

Use of Eq. (18) in Eq. (15) yields

$$\begin{aligned} \sigma^2_{(tot)}(L_m) &= (K_{2m-1} - 1)\sigma^2_{cc,1}(L_m) \\ &+ \frac{2}{6}K_{2m-1}\sigma^2_{cc,1}(L_m) \\ &= (\frac{4}{3}K_{2m-1} - 1)\sigma^2_{cc,1}(L_m). \end{aligned} \qquad (19)$$

Recall that K_1 denotes the maximum number of users for the single channel case such that the prespecified probability of error for each user is not exceeded. So that this condition on the probability of error holds for the present case of overlapping sub-channels it is necessary that

$$\sigma^2_{(tot)}(L_m) \le \sigma^2_{cc,(K_1-1)}(L_1)$$
$$(\frac{4}{3}K_{2m-1} - 1)\sigma^2_{cc,1}(L_m) \le (K_1 - 1)\sigma^2_{cc,1}(L_1)$$
$$K_{2m-1} \le \frac{3}{4}[(K_1 - 1)\frac{\sigma^2_{cc,1}(L_1)}{\sigma^2_{cc,1}(L_1/m)} + 1]. \qquad (20)$$

This requires that the ratio $\sigma^2_{cc,1}(L_1)/\sigma^2_{cc,1}(L_1/m)$ be known. Determining this ratio requires evaluation of Eq. (11) for L_1 and L_1/m An analytical expression for $\sigma^2_{cc,1}(L_1)/\sigma^2_{cc,1}(L_1/m)$ is very cumbersome. Hense, $\sigma^2_{cc,1}(L_1/m)/\sigma^2_{cc,1}(L_1)$ is plotted versus m in Fig. 3 to get an idea of how this ratio varies with m. Note from Fig. 3 that the relationship is approximately a straight line with 45° slope. Hence,

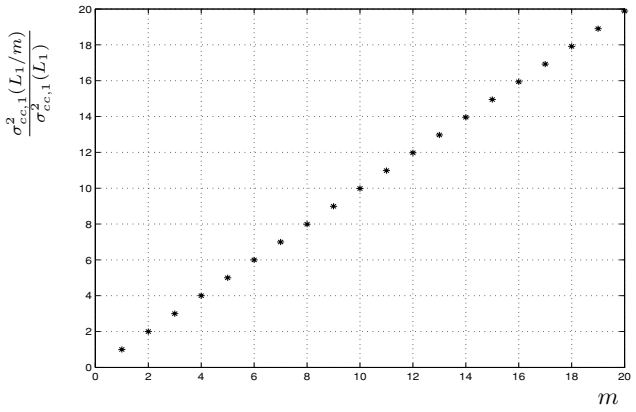

Figure 3: Plot of the ratio $\sigma^2_{cc,1}(L_1/m)/\sigma^2_{cc,1}(L_1)$ as a function of m

$$\frac{\sigma^2_{cc,1}(L_1/m)}{\sigma^2_{cc,1}(L_1)} \approx m. \qquad (21)$$

Substitution of Eq. (21) into Eq. (20) yields the conclusion that K_{2m-1} is the maximum integer such that

$$K_{2m-1} \le \frac{3}{4}[\frac{(K_1 - 1)}{m} + 1]. \qquad (22)$$

Since there are (2m-1) sub-channels, the maximum number of users is the largest integer such that

$$K_{T,(2m-1)} = (2m-1)K_{2m-1}$$
$$\le \frac{3}{4}\frac{(2m-1)}{m}[K_1 - 1 + m]. \qquad (23)$$

To verify the analytical results and to gauge the accuracy of the simplified worst-case approach, a Monte Carlo computer simulation was carried out. Due to limitations of the computing resources, the simulation assumes that the processing gains and frequencies used for the simulation are smaller than those used in actual practice. Fig. 4 depicts a DSSS channel of bandwidth B_1 = 12 kHz. It is assumed that the processing gain is L_1 =60 and there are a total of 78 users for the simulation. The probability of error for this case obtained from the computer simulation is 0.064. Letting m=3, the channel of Fig. 4 was subdivided into five overlapping sub-channels of equal bandwidth as shown in Figure 5. With

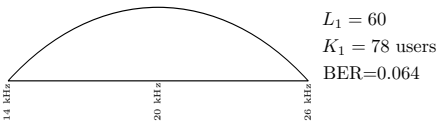

Figure 4: DSSS channel before subdivision

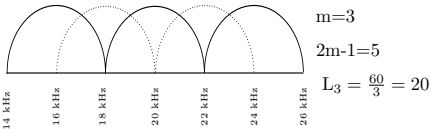

Figure 5: DSSS channel after subdivision when m=3

reference to Eq. (23), the maximum number of users that can be allocated within each sub-channel is the largest integer such that

$$K_5 \le \frac{3}{4}[\frac{(78-1)}{3} + 1]$$
$$\le 20. \qquad (24)$$

Hence, K_5 = 20. Using a Monte Carlo simulation, the probability of error with 20 users for each sub-channel was found to be 0.0544. The smaller probability of error is believed to be due to the worst case approach used in the analysis. The total number of users within the entire channel is the sum of the users in the individual sub-channels. Therefore, there will e a total of 5x20=100 users. When the channel was not subdivided, the number of users was 78. This is an increase of 28.3%. As shown in Fig. 6, this procedure was repeated for m=4. Making

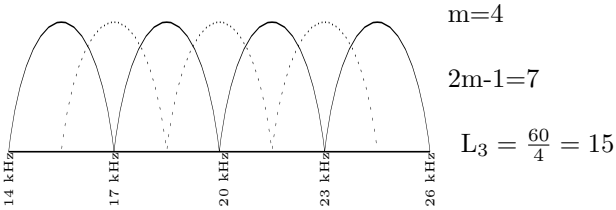

Figure 6: DSSS channel after subdivision when m=4

Use of Eq. (23) $K_{2m-1} = K_7$ is the largest integer such that

$$K_7 \le \frac{3}{4}[\frac{(78-1)}{4} + 1]$$
$$= 15.1875 \qquad (25)$$

Thus, K_7 = 15. Using a Monte Carlo simulation, the probability of error is found to be 0.0413. Once again, the effect of our worst-case approach is seen. This yields an increase in the number of users by 34.6 % even with our worst-case approach. Table (1) summarizes the results for m=1,3,4,5, and 6. Note that the percentage increase in users grows with m. The limiting case with increasing m occurs for m = 60. This results in 119 users or an increase of 52.69%.

IV. Conclusion

As the number of users is increased, performance of the conventional DSSS system becomes an issue. Hence, we proposed a novel approach that can provide a significant increase in the number of users in a given bandwidth over that presently available. The proposed technique is based on division of the entire channel into a

number of sub-channels having a smaller bandwidth than the entire channel bandwidth. Analytical results were obtained to estimate the number of users when the channel is divided into smaller bandwidth sub-channels. It is seen from the analytical results and computer simulations that the proposed approach allows more users to be accommodated than is now possible with the conventional single carrier DSSS system.

m	$L_m = \frac{L_1}{m}$	$2m-1$	K_{2m-1}	$(2m-1)K_{2m-1}$	BER	% Improvement
1	60	1	78	78	0.0640	0
3	20	5	20	100	0.0544	28.1
4	15	7	15	105	0.0413	34.6
5	12	9	12	108	0.0614	38.4
6	10	11	10	110	0.0531	41.1

Table 1: Increase in Number of Users for Overlapping Sub-channels

References

[1] Ilteris Demirkiran, "Simplified Analysis of Electromagnetic Interference in Weakly Nonlinear and Spread Spectrum Systems,". PhD dissertation, Syracuse University, 2004.

[2] Ilteris Demirkiran, Donald D. Weiner, Pramod K. Varshney, " A General Approach for Performance Evaluation of Multi-user Direct-Sequence Spread Spectrum (DSSS) Systems." The 2004 Conference on Information Sciences and Systems (CISS), Princeton, NJ, March 2004. EMC

2007 International Waveform Diversity & Design Conference

June 4 - 8, 2007 Pisa, Italy
Keynote Speaker: Dr. Alfonso Farina

Organizing Committee:

General Chairs
Prof. Vinny Amuso, USA
Prof. Maria Greco, Italy
Technical Chairs
Dr. Eric Mokole, USA
Prof. Chris Baker, UK
Publicity Chair
Prof. Shannon Blunt, USA
Tutorial Chair
Maj. Todd Hale, USA
Student Involvement Chair
Prof. Eli Saber, USA
Awards Chair
Prof. Hugh Griffiths, UK

Recent advances in hardware technology are enabling a much wider range of design freedoms to be explored for sensor and communication systems. As a result, there are emerging and compelling changes in system requirements, such as more efficient spectrum usage, higher sensitivities, transmitter/receiver agility, greater information content, improved robustness to errors, etc. The combination of these is fueling a worldwide interest in the subject of waveform design and the use of waveform diversity techniques. This third conference in the ongoing series will continue to build on the success of the previous two conferences by bringing together researchers from numerous diverse backgrounds and specialties to facilitate the exchange and cross-fertilization of ideas and research. The WDD organizing committee invites original contributions to Waveform Diversity and Design in the general areas of Communications, Radar, Sonar, etc. Specifically, topics to be included are:

Radar Systems
Sonar Systems
3G/4G Communication Systems
Laser Systems
Interference Suppression
RF Compatibility
Space-Time Adaptive Processing
Channel Estimation/Equalization
Software Agile Radio/Radar
Passive Sensing Operation
Target-Adaptive Matched Filtering
Multi-function Operation
Impulsive Systems
Tomography
Ultra-wideband Operation
Target Detection
Tracking
Interferometry
SAR/ISAR
MIMO Communications
RF Hitchhiking
Error Correction Coding
Modulation Schemes
Multiple-access Schemes
Multi-user Operation
Bandwidth-on-Demand Synchronization
RF Imaging
Hardware Efficiency
Bi-static/multi-static Operation
Sensor Fusion
Polarimetry
EM Phenomenology

Abstracts of 1,000 - 1,500 words are solicited which should include examples of data and illustrations. Send abstracts to the Conference organizer at WaveformDiversity@rl.af.mil in Word 97 or later, or (preferably) PDF format before 8 December 2006. Receipt of abstracts will be acknowledged by e-mail. Conference organizer contact: Patricia Woodard, (315) 330-2215. Additional information is available at http://www.waveformdiversity.org. Authors of accepted papers will be notified by 9 February 2007 and will receive instructions for publication at that time. Complete papers of a maximum of five pages (including text and illustrations) will be required by 30 March 2007.

Dates to Remember:
Abstracts Due - 8 Dec 2006
Notification of Acceptance of Papers - 9 Feb 2007
Final Papers Due - 30 Mar 2007